THE JOURNAL OF BIOLOGICAL CHEMISTRY
Vol. 276, No. 37, Issue of September 14, pp. 35060–35070, 2001
Printed in U.S.A.

RICH, a Rho GTPase-activating Protein Domain-containing Protein Involved in Signaling by Cdc42 and Rac1*

Received for publication, April 20, 2001, and in revised form, June 21, 2001
Published, JBC Papers in Press, June 28, 2001, DOI 10.1074/jbc.M103540200

Ninna Richnau and Pontus Aspenström‡

From the Ludwig Institute for Cancer Research, Biomedical Center, Box 595, S-751 24 Uppsala, Sweden

A previously unidentified Rho GTPase-activating protein (GAP) domain-containing protein was found in a yeast two-hybrid screen for cDNAs encoding proteins binding to the Src homology 3 domain of Cdc42-interacting protein 4 (CIP4). The protein was named RICH-1 (*R*hoGAP *i*nteracting with *C*IP4 *h*omologues), and, in addition to the RhoGAP domain, it contained an N-terminal domain with endophilin homology and a C-terminal proline-rich domain. Transient transfections of RICH-1 indicated that it bound to CIP4 *in vivo,* as shown by co-immunoprecipitation experiments, as well as co-localization assays. *In vitro* assays demonstrated that the RhoGAP domain of RICH-1 catalyzed GTP hydrolysis on Cdc42 and Rac1, but not on RhoA. Ectopic expression of the RhoGAP domain as well as the full-length protein interfered with platelet-derived growth factor BB-induced membrane ruffling, but not with serum-induced stress fiber formation, further emphasizing the notion that, *in vivo,* RICH-1 is a GAP for Cdc42 and Rac1.

The cytoskeleton is a major determinant for eukaryotic cell function. The cytoskeleton is formed by three distinct filament systems, the microfilament system, the intermediate filament system, and the microtubule system, which act in concert to orchestrate processes such as cell locomotion, changes in cell morphology, and intracellular transport (1, 2). Cytoskeletal elements, in particular, the microfilament system, are under a constant reconstruction in response to external stimuli. There exists a close correlation between the activation of transmembrane receptors as well as cell adhesion molecules and the mobilization of the microfilament system (1, 2). Actin monomers, which polymerize into asymmetric filaments, form the core of the microfilament system. In addition, a large number of actin-binding proteins assist in organization of actin filaments in a variety of supramolecular structures.

A family of signaling intermediates, the Rho GTPases, has been shown to be a pivotal regulator of the microfilament system and thereby of the morphogenetic and motile properties of mammalian cells. Each member of the archetypal trio of Rho GTPases, RhoA, Rac1, and Cdc42, has been found to regulate distinct actin filament-containing structures. Rho regulates the formation of focal adhesions and the subsequent assembly of stress fibers, and Rac regulates the formation of membrane lamellae, whereas Cdc42 triggers the outgrowth of peripheral spike-like protrusions called filopodia (3, 4). The potential of the Rho GTPases to function as signaling switches resides in their ability to cycle between active, GTP-bound states and inactive, GDP-bound states. This cycling is orchestrated by guanine nucleotide exchange factors, GTPase-activating proteins (GAPs),[1] and guanine nucleotide dissociation inhibitors. Guanine nucleotide exchange factors stimulate the replacement of GDP by GTP, whereas GAPs stimulate the intrinsic GTP hydrolysis of the GTPase (5–7). Guanine nucleotide dissociation inhibitors act by blocking GDP dissociation, and, in resting cells, the Rho GTPases are thought to reside in an inactive complex with guanine nucleotide dissociation inhibitor proteins (7, 8). Recent work has revealed that, in mammals, the Rho family consists of at least 16 distinct members that can be further divided into six subgroups: Cdc42 (Cdc42, TC10, TCL, and Chp), Rac (Rac1–3 and RhoG), Rho (Rho A-C), Rnd (Rnd1–2 and RhoE), RhoD, and RhoH (9, 10). Moreover, the Rho GTPases have been shown to regulate several vital cellular processes in addition to cytoskeletal rearrangements. Rac and Cdc42 participate in transcriptional control via the Jun N-terminal kinase/stress-activated protein kinase and $p38^{MAPK}$ signaling cascades, Rho has a role in serum response factor-regulated gene transcription, and all three contribute to transcriptional activation via the nuclear factor κB signaling pathway (4, 10–15). Furthermore, the Rho GTPases are also participants in signaling leading to cell cycle entry and apoptosis (4, 13).

The identification of binding partners for the Rho GTPases has resulted in insights into the mechanisms by which these proteins mobilize the microfilament system (4, 14, 15). A major advancement in our understanding originates from the work on the Wiskott-Aldrich syndrome protein (WASP) family of proteins, which have emerged as important regulators of actin assembly in eukaryotic cells (16, 17). This family of proteins also includes N-WASP and Scar/WAVE 1–3 (18). WASP was originally identified as the gene defective in the rare immunodeficiency disorder Wiskott-Aldrich syndrome (19, 20). WASP is a multidomain adapter protein that contains a phosphoinositide-binding domain, a Cdc42/Rac interactive binding (CRIB) domain that specifically binds Cdc42 (21), and an extended proline-rich domain that binds SH3 domain-containing proteins such as Nck, Src, and Btk/Tec (18). Moreover, it was recently found that the members of the WASP family bind directly to actin and to the so-called Arp2/3 complex. This

* This work was supported in part by grants from the Swedish Cancer Foundation (to P. A.). The costs of publication of this article were defrayed in part by the payment of page charges. This article must therefore be hereby marked "*advertisement*" in accordance with 18 U.S.C. Section 1734 solely to indicate this fact.

The nucleotide sequence(s) reported in this paper has been submitted to the GenBank™/EBI Data Bank with accession number(s) AJ306731 (RICH-1) and AJ306732 (RICH-1B).

‡ To whom correspondence should be addressed. Tel.: 46-18-160408; Fax: 46-18-160420; E-mail: pontus.aspenstrom@LICR.uu.se.

[1] The abbreviations used are: GAP, GTPase-activating protein; CIP4, Cdc42-interacting protein 4; CRIB, Cdc42/Rac interactive binding; FITC, fluorescein isothiocyanate; HA, hemagglutinin; PDGF, platelet-derived growth factor; SH3, Src homology 3; TRITC, tetramethyl rhodamine isothiocyanate; WASP, Wiskott-Aldrich syndrome protein; bp, base pair(s); GST, glutathione *S*-transferase; DTT, dithiothreitol; PBS, phosphate-buffered saline; EGFP, enhanced green fluorescent protein.

multisubunit protein complex has an essential role in regulating actin polymerization in cells. It is suggested that Arp2/3 is needed for both the formation of new actin filaments and binding to the sides of actin filaments, thereby forming branched actin filament networks (16–18).

Several other Cdc42-binding proteins have been found to affect the organization of the actin cytoskeleton, although the mechanisms by which they act are less well known. A common denominator for most of these proteins is the presence of a CRIB domain (21). For instance, MSE55 has been shown to induce filopodia-like protrusions when overexpressed in fibroblasts (22), whereas some of the five known MSE55-related Borg (binders of Rho GTPases) proteins have been suggested to function as negative regulators of Rho (23). The SPEC-1/2 (small protein effectors of Cdc42) proteins induce an accumulation of polymerized actin in peripheral membrane protrusions in fibroblasts (24). Cdc42-interacting protein 4 (CIP4), however, binds Cdc42 via a domain motif unrelated to the CRIB domain (25). Overexpression of CIP4 in fibroblasts leads to the disappearance of filamentous actin bundles in these cells. Moreover, simultaneous expression of activated Cdc42 and CIP4 results in a relocalization of the uniformly distributed CIP4 into peripheral and dorsal clusters or villi-like structures, which might represent precursors of filopodia (25).

To elucidate the mechanisms by which CIP4 acts, we sought to identify binding partners for the protein. A yeast two-hybrid screen identified a previously uncharacterized RhoGAP domain-containing protein that specifically interacted with the SH3 domain of CIP4. We named this protein RICH-1 (*R*hoGAP *i*nteracting with *C*IP4 *h*omologues). The N-terminal portion of RICH-1, including the RhoGAP domain, was shown to be homologous to a protein of unknown function, KIAA0672, which we propose should be renamed RICH-2. The RhoGAP domain of RICH-1 was furthermore shown to be similar to the analogous domain of the Abl-binding protein 3BP-1 (26). The high degree of similarity between the proteins suggested that RICH-1, RICH-2, and 3BP-1 form a closely related family of RhoGAPs. *In vitro* assays demonstrated that the RhoGAP domains of RICH-1 and RICH-2 specifically activate the GTP hydrolysis of Rac1 and Cdc42, but not of RhoA. Ectopic expression of the RhoGAP domain of RICH-1 abrogated PDGF-BB-induced membrane ruffles but not the serum-induced stress-fibers, further emphasizing the notion that RICH-1 is a Rac and Cdc42-specific GAP.

EXPERIMENTAL PROCEDURES

DNA Work and Yeast Two-hybrid System Screen—The *Saccharomyces cerevisiae* strain Y190 (genotype, MATa, *gal4–542*, *gal80–538*, *his3*, *trp1–901*, *ade2–101*, *ura3–52*, *leu2–3, 112*, URA3::GAL1-LacZ, Lys2::GAL1-HIS3cyh^r) was transformed with a cDNA encoding the SH3 domain of CIP4 (amino acid residues 489–545) fused to the GAL4 DNA-binding domain in the pYTH6 vector. This GAL4 DNA-binding domain-CIP4:SH3-expressing yeast strain was used to screen a cDNA library from Epstein-Barr virus-transformed human B cells fused to the GAL4 activation domain in the pACT vector as described previously (25, 27). Thirteen clones encoding potential CIP4-interacting proteins were isolated, one of which encoded a partial cDNA for a previously uncharacterized RhoGAP domain-containing protein, which was subsequently named RICH-1. This yeast two-hybrid clone represented a fragment that was later found to encode amino acid residues 387–803 of the full-length polypeptide. The partial clone was used to screen a human brain λ ZAP II cDNA library following standard procedure (28). Clones (9×10^6) were screened, and three positive clones were isolated after rescreening. These clones were recovered as phagemid Bluescript SK$^-$ constructs by excision from the λ vector with helper phage R408 as described in Ref. 29. One of the clones contained a putative initiator codon; however, the predicted amino acid sequence stopped prematurely before the RhoGAP domain, resulting in an open reading frame of 226 amino acid residues. Polymerase chain reaction was employed to screen various cDNA libraries for splice variants of RICH-1 that encoded a RhoGAP domain-containing protein. The presence of a splice variant encoding an insert of an extra 82 bp was detected in human B cells as well as in HeLa cells. This splice variant encoded a protein with an open reading frame of 803 amino acid residues. We designated the long form RICH-1 and the short form RICH-1B. The nucleotide sequences of RICH-1 and RICH-2 have been deposited in the EMBL data base with the accession numbers AJ306731 (RICH-1) and AJ306732 (RICH-1B).

Fragments of RICH-1, RICH-1B, and RICH-1 RhoGAP domain were generated as *Bam*HI-*Eco*RI polymerase chain reaction fragments and inserted into the pRK5myc vector. The C-terminal domain of RICH-1 (amino acids 384–803) was subcloned into the *Hin*dIII and *Eco*RI sites of the pEGFP-C3 vector. The SH3 domains of CIP4 (amino acid residues 489–545), forming-binding protein 17 (amino acid residues 550–617), and syndapin (amino acid residues 376–441) were subcloned into the pGEX-2T vectors. DNA sequencing on a Perkin Elmer Genetic Analyzer 310 confirmed the fidelity of the nucleotide sequence. The DNA work followed standard procedures (28).

Sequential deletion mutants of RICH-1 lacking the proline-rich motives were generated by polymerase chain reaction (see Fig. 5 for a detailed description) and subcloned into the pRK5myc vector. The arginine to alanine mutation of RICH-1 in codon 288 (RICH-1R288A), which rendered the protein catalytically inactive, was generated by the QuikChange site-directed mutagenesis kit (Stratagene).

Northern Blot Analysis—Probes representing DNA fragments encoding amino acid residues 387–803 of RICH-1, amino acid residues 1–818 of RICH-2, and the 82-bp insert uniquely present in RICH-1 were labeled with [^{32}P]CTP using the rediprime labeling kit (Amersham Pharmacia Biotech). The probes were then hybridized to hybridization-ready Northern blots (Human Multiple Tissue Northern blot; CLONTECH) according to the ExpressHyb (CLONTECH) protocol provided by the manufacturer.

Protein Production—Glutathione *S*-transferase (GST) fusion proteins of Rac1, Cdc42 (brain isoform), and RhoA were expressed in *Escherichia coli*, purified on glutathione-Sepharose beads (Amersham Pharmacia Biotech), and isolated from GST fusion proteins by thrombin cleavage as described previously (25, 30). GST fusion proteins of the RhoGAP domains of RICH-1 (amino acid residues 221–489), RICH-2 (KIAA0672 obtained from the Kazusa DNA Research Institute, Chiba, Japan; amino acids residues 217–469), and p50^{RhoGAP} (amino acid residues 230–439) were expressed in *E. coli*. The bacteria were lysed in a buffer containing 50 mM Tris-HCl, pH 7.5, 5 mM $MgCl_2$, 50 mM NaCl, 10% glycerol, 0.1% Triton X-100, 1 mM phenylmethylsulfonyl fluoride, 1% aprotinin (Trasylol; Beyer), and 1 mM dithiothreitol (DTT). The proteins were then eluted from the glutathione-Sepharose beads with 5 mM reduced glutathione, desalted on PD10 prepacked chromatography columns (Amersham Pharmacia Biotech), equilibrated in 20 mM Tris-HCl, pH 7.5, 10% glycerol, and 1 mM DTT, and concentrated using Centricon-10 (Millipore). Protein concentrations were determined according to the Bradford method. GST fusion proteins of the SH3 domains described in Fig. 4*A* were prepared as described above but were retained on the glutathione-Sepharose beads.

GTPase Activation and Nucleotide Exchange Assays—The procedure we used essentially followed the procedure described by Self and Hall (31). Briefly, 0.1 μg of recombinant wild-type Rac, Rho, or Cdc42 was preloaded with 10 μCi of [γ-^{32}P]GTP (Amersham Pharmacia Biotech) in 20 μl of 20 mM Tris-HCl, pH 7.5, 25 mM NaCl, 5 mM EDTA, and 0.1 mM DTT. The mixture was incubated for 10 min at 30 °C, and then the reaction was terminated by adding 5 μl of 0.1 M $MgCl_2$, and the resulting [γ-^{32}P]GTP-loaded GTPase solutions were stored on ice. For the GAP assays, equimolar amounts of the GTPases and the GST-GAP domains were used. Three μl of the [γ-^{32}P]GTP-loaded GTPase was added to a 30-μl mixture of 20 mM Tris-HCl, pH 7.5, 1 mM nonradioactive GTP, 0.87 mg/ml bovine serum albumin, and 0.1 mM DTT with the GST-RhoGAP domains of either RICH-1, RICH-2, or p50^{RhoGAP}. The mixture was incubated at 30 °C, 5-μl aliquots were removed after 0, 3, 6, 9, and 15 min, and the reaction was stopped by the addition of 1 ml of ice-cold buffer A (50 mM Tris-HCl, pH 7.5, 50 mM NaCl, and 5 mM $MgCl_2$). The samples were collected on nitrocellulose filters and washed with 10 ml of ice-cold buffer A, and the portion of [γ-^{32}P]GTP remaining bound to the GTPases was determined by scintillation counting. For the exchange assays, a similar protocol was employed, but 0.5 mCi of [8-^{3}H]GTP (Amersham Pharmacia Biotech) was used instead.

Cell Cultivation, Transfection, GST Pull-down Assays, and Immunoprecipitation—Cos-1, Swiss 3T3, and NIH 3T3 cells were cultured in Dulbecco's modified Eagle's medium supplemented with 10% fetal calf serum (10% calf serum for NIH 3T3 cells) and penicillin/streptomycin at 37 °C in an atmosphere of 5% CO_2. Porcine aortic endothelial cells

stably expressing the PDGF-β receptor (clone PAE/PDGFRβ) were cultured in Ham's F-12 medium supplemented as described above. For the characterization of antisera, transiently transfected Cos-1 cells were metabolically labeled for 4 h at 37 °C with 15 μCi/ml Easy Tag EXPRESS ^{35}S protein labeling mix in MCDB 104 medium lacking cysteine and methionine and supplemented with HEPES. Cos-1 cells were transfected according to the DEAE-dextran method (32). Transfected cells were harvested 48 h after transfection, washed once in ice-cold PBS, and lysed on ice in Nonidet P-40 buffer (20 mM HEPES, pH 7.5, 150 mM NaCl, 10% glycerol, 1% Nonidet P-40, 1 mM phenylmethylsulfonyl fluoride, 1% aprotinin (Trasylol; Beyer) and 1 mM DTT). Lysed cells were collected in Eppendorf tubes and centrifuged for 15 min. The resulting supernatants were subjected to immunoprecipitation experiments or GST pull-down assays. For co-immunoprecipitations of HA epitope-tagged CIP4 and myc epitope-tagged RICH-1, supernatants were incubated together with antibodies as indicated in the figure legends for 1 h at 4 °C, after which immunoprecipitates were collected on protein G-Sepharose 4 Fast Flow (Amersham Pharmacia Biotech). The beads were washed three times with Nonidet P-40 buffer, and SDS-polyacrylamide gel electrophoresis sample buffer was added to each sample. The immunoprecipitates as well as control cell lysates were subjected to SDS-polyacrylamide gel electrophoresis, and the proteins were then transferred to Immobilon-P filters (Millipore). Western blots were detected by the BM chemiluminescence blotting substrate (Roche Molecular Biochemicals). The ^{35}S-labeled RICH-1 immunoprecipitates were subjected to SDS-polyacrylamide gel electrophoresis, and the gels were fixed for 15 min in 25% methanol and 7.5% acetic acid and soaked in Amplify (Amersham Pharmacia Biotech) for 30 min. The gels were then dried and exposed on a phosphorimager (Fujix BAS 2000). For GST pull-down assays, supernatants from lysed RICH-1-transfected Cos-1 cells were incubated with GST fusion proteins of SH3 domains from a panel of proteins described in Fig. 4*A,* and the presence of RICH-1 bound to the GST fusion protein was determined by Western blotting. For immunocytochemical analysis, Swiss 3T3 cells, NIH 3T3 fibroblasts, or PAE/PDGFRβ cells were seeded on coverslips and transfected by LipofectAMINE Plus (Life Technologies, Inc.) according to the protocols provided by the manufacturer.

Determination of GTP Loading on Rho GTPases—GST fusion proteins of the PAK-CRIB and WASP-CRIB domains encompassing amino acids 56–267 and 201–321 of PAK1B and WASP, respectively, were purified essentially as described in Ref. 33. PAE/PDGFRβ cells were transiently transfected with pRK5mycCdc42 or pRK5mycRac1 in combination with the pRK5mycRICH-1 RhoGAP domain or pRK5myc encoding the catalytically inactive R288A mutant RICH-1 RhoGAP domain. Forty-eight h after transfection, the cells were washed with ice-cold PBS supplemented with 1 mM $MgCl_2$. The cells were then lysed on ice in a cold room with a buffer containing 50 mM Tris-HCl, pH 7.5, 1% Triton X-100, 0.5% sodium deoxycholate, 0.1% SDS, 0.5 M NaCl, 10 mM $MgCl_2$, 1% aprotinin, and 1 mM phenylmethylsulfonyl fluoride. The cell lysates were immediately subjected to centrifugation. Active, GTP-bound Rac1 and Cdc42 were isolated from the supernatants by the addition of GST-PAK-CRIB and GST-WASP-CRIB, respectively, followed by a 10-min incubation. The beads were washed three times with a buffer containing 50 mM Tris-HCl, pH 7.5, 1% Triton X-100, 150 mM NaCl, 10 mM $MgCl_2$, 1% aprotinin, and 1 mM phenylmethylsulfonyl fluoride. Equal amounts of proteins were subjected to SDS-polyacrylamide gel electrophoresis, and the extent of GTP-bound Cdc42 and Rac1 was determined by Western blotting.

Antibodies and Immunocytochemistry—Antisera were raised against peptides representing amino acid residues 53–67 (antiserum N) and 779–792 (antiserum C) of human RICH-1. These antisera, as well as mouse anti-myc (9E10; Santa Cruz Biotechnology), mouse anti-HA (12CA5; Roche Molecular Biochemicals), rabbit anti-green fluorescent protein (CLONTECH), and tetramethyl rhodamine isothiocyanate (TRITC)- and fluorescein isothiocyanate (FITC)-conjugated anti-rabbit and anti-mouse antibodies (DAKO), were used for immunoprecipitations and to determine the subcellular localization of CIP4 and RICH-1 mutants. Filamentous actin was visualized by TRITC- or FITC-conjugated phalloidin (Sigma). For immunocytochemistry assays, the cells were grown on coverslips and fixed in 2% paraformaldehyde in PBS for 20 min. The cells were washed with PBS and permeabilized in 0.2% Triton X-100 in PBS for 5 min. The cells were then washed again and incubated in the presence of 10 mM glycine in PBS for 1 h. Primary as well as secondary antibodies were diluted in PBS containing 5% fetal calf serum. Cells were incubated with primary antibodies followed by secondary antibodies for intervals of 1 h, with a washing step in between. The coverslips were mounted in Fluoromount-G (Southern Biotechnology Associates, Inc.) on object slides. Cells were photographed by a Hamamatsu ORCA charge-coupled device digital camera employing the QED Imaging System software using a Zeiss Axioplan2 microscope.

RESULTS

Isolation of RICH as a CIP4-binding Protein—The yeast two-hybrid system was used to identify binding partners for CIP4. In a screen, employing the SH3 domain of CIP4 as bait, 13 CIP4-interacting clones were isolated from a cDNA library from Epstein-Barr virus-transformed human B cells. Data base searches showed that one of the clones represented a partial cDNA of a previously unidentified RhoGAP domain-containing protein, which we named RICH-1. This clone lacked a putative transcriptional start site; therefore, the partial cDNA was used to screen a λ ZAP II human brain cDNA library. Three positive clones were recovered, one of which contained a putative initiator codon in agreement with the Kozak consensus (34). Surprisingly, the predicted open reading frame resulted in a protein of only 226 amino acids, terminating immediately upstream of the RhoGAP domain. This suggested the existence of alternative splice variants of RICH. The polymerase chain reaction revealed the occurrence of an 82-bp insert located upstream of the RhoGAP domain in RICH cDNAs from human B cells and HeLa cells. The presence of this insert resulted in a transcript with a considerably longer open reading frame of 803 amino acid residues (Fig. 1*A*). The insert could not be detected in brain-derived cDNAs (see also Fig. 2*B*). We named the 803- and 226-amino acid residue splice variants RICH-1 and RICH-1B, respectively (Fig. 1*B*).

Domain Structure of RICH-1—RICH-1 exhibited extensive similarity to a protein with the annotation KIAA0672, identified by the Kazusa DNA Research Institute. Due to the similarity between the two proteins, we suggest that KIAA0672 should be renamed RICH-2. These two proteins also displayed a high degree of similarity to the c-Abl-interacting protein 3BP-1, suggesting that the three proteins form a closely related family of RhoGAP proteins. RICH-1 and RICH-2 both contain an N-terminal domain with homology to the endophilin family of proteins (Fig. 1, *B* and *D*) (35). RICH-1B encompasses only the endophilin-like domain, suggesting that this part of the protein has a unique but as yet unknown function. Data base searches against the nucleotide sequences released by the Human Genome Project indicate that 3BP-1 also contains a similar domain, which was not reported in the original publication of the 3BP-1 amino acid sequence (36).[2] Multiple alignment of the central RhoGAP domains of RICH-1, RICH-2, and 3BP-1 demonstrated that they all contain the conserved arginine finger, which is present in this type of domain (Fig. 1*C*) (6, 7). The mutual similarity between RICH-1, RICH-2, and 3BP-1 is restricted to the endophilin-like and RhoGAP domains because their C termini are divergent. RICH-2 and 3BP-1 each contain one proline-rich motif, whereas RICH-1 contains four proline-rich sequences (Fig. 1*E*). The spacing between the individual proline-rich motifs indicates that RICH-1 can bind multiple SH3 domain-containing proteins (6, 37).

Tissue Distribution of RICH-1—A commercial human multiple tissue Northern blot was hybridized with a probe derived from the 3′ part of RICH-1. A transcript of ~4 kilobases was present in all tissues analyzed (Fig. 2*A*), indicating that RICH-1 is ubiquitously expressed; however, the expression was particularly high in the heart and placenta. This expression pattern most likely represents the combined distribution of RICH-1 and RICH-1B because they differ only by the presence of the 82-bp insert in RICH-1. To study the distribution of RICH-1 alone, we rehybridized the filter with a probe representing the 82-bp insert (Fig. 2*B*). The expression pattern is

[2] P. Aspenström, unpublished observation.

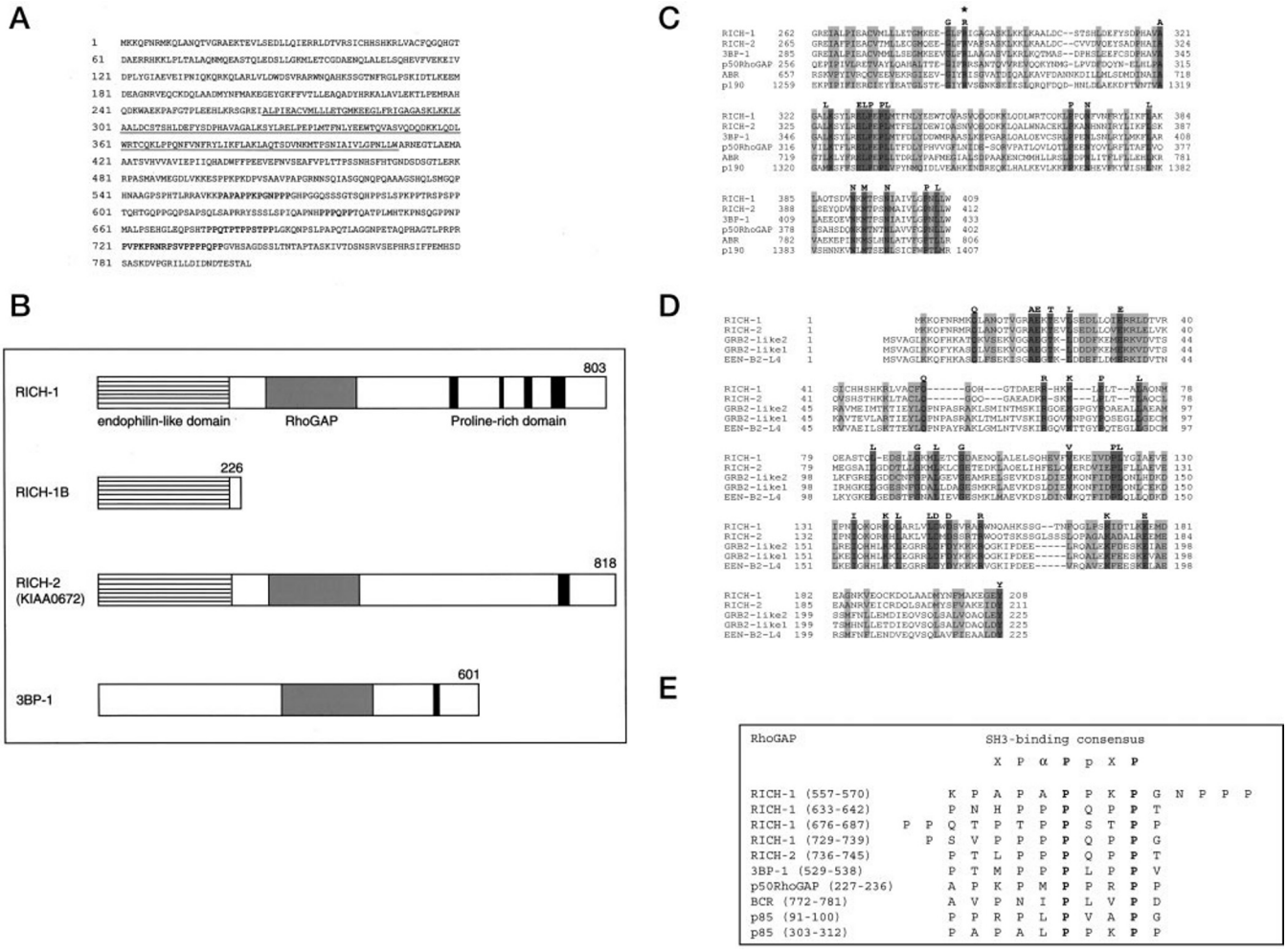

FIG. 1. **Domain structure of RICH.** *A,* amino acid sequence of RICH-1. The RhoGAP catalytic domain is *underlined,* and the proline-rich regions are shown in *bold*. *B,* schematic representation of RICH-1, RICH-1B, and the related proteins RICH-2 (KIAA0672) and 3BP-1. *C,* sequence alignment with the assistance of the DNAssist program of RhoGAP domains of RICH-1, RICH-2, 3BP-1, p50^{RhoGAP}, ABR (active Bcr-related), and p190^{RhoGAP} (α isoform). Identical amino acid residues are indicated in *bold,* and the critical arginine is marked with an *asterisk*. *D,* sequence alignment with the assistance of the DNAssist program of the N-terminal domains of RICH-1, RICH-2, and members of the endophilin family called SH3 domain GRB2-like 1, SH3 domain GRB2-like 2, and EEN-B2-L4 (GenBank^{TM} accession numbers NM_003025.1, NM_003026.1, and AF036272.1). The identical residues are indicated in *bold*. *E,* sequence alignment of the proline-rich regions in RICH-1, RICH-2, 3BP-1, p50^{RhoGAP}, Bcr (break point cluster region), and p85 (p85α subunit of the phosphoinositide 3′-kinase) with a SH3-binding motif consensus sequence. *X,* nonconserved residue; *p,* proline preferred; α, hydrophobic residue; ***P,*** conserved proline.

similar to that in Fig. 2*A,* however, RICH-1 appeared to be more abundantly expressed in skeletal muscle and was almost absent from the brain. We also performed a Northern blot with a RICH-2-specific probe (Fig. 2*C*). This protein is expressed at low levels in all tissues tested; however, the expression was pronounced in the brain, where the RICH-1 expression was very low.

Peptides encompassing amino acid residues 53–67 and 779–792 of RICH-1 were used to generate antiserum N and antiserum C, respectively. The specificity of the antisera was tested by immunoprecipitating RICH-1, RICH-1B, or RICH:384–803 from transiently transfected, ^{35}S-labeled Cos-1 cells. Antiserum N effectively precipitated RICH-1 and RICH-1B, and antiserum C effectively precipitated RICH-1 and RICH:384–803 (Fig. 3).

Binding Partners for RICH-1—To test the interaction between RICH-1 and CIP4 and identify additional potential binding partners for the C-terminal proline-rich motifs of RICH-1, we performed GST pull-down experiments with GST fusion proteins from a panel of different SH3 domains. Cos-1 cells expressing EGFP-RICH-1:384–803 were lysed, and the protein was precipitated with the different SH3 domains as indicated in Fig. 4*A*. Under these conditions RICH-1 bound to several of the SH3 domains; however, particularly strong binding was found between RICH-1 and the SH3 domains of CIP4, formin-binding protein 17, and syndapin (these latter proteins are related to CIP4).

To confirm the interaction between RICH-1 and CIP4 *in vivo,* Cos-1 cells were transiently transfected with plasmids encoding EGFP-RICH-1:384–803 and either the full-length HA epitope-tagged CIP4 or a CIP4 mutant lacking the SH3 domain. RICH-1:384–803 bound only to the intact CIP4, emphasizing the importance for the SH3 domain of CIP4 for mediating the interaction to RICH-1 (Fig. 4*B*). We also tested the interaction between full-length RICH-1 and CIP4 by expressing myc epitope-tagged RICH-1 and HA epitope-tagged CIP4 in Cos-1 cells. CIP4 was detected in RICH-1 immunoprecipitates (Fig. 4*C*).

CIP4 Binds to the Second Proline-rich Motif of RICH-1—To identify which of the four proline-rich motifs mediated CIP4 binding, a series of RICH-1 mutants were produced by sequentially deleting one proline-rich motif after the other (Fig. 5*A*). Cos-1 cells were transiently transfected with plasmids encoding either full-length RICH-1 or the deletion mutants. The RICH-1 variants were tested in a GST pull-down assay employing the GST-CIP4-SH3 domain. Mutant RICH-1 lacking the

proline-rich motifs 3 and 4 still bound to the SH3 domain of CIP4; however, when the second proline-rich motif was deleted, the interaction with CIP4 was lost (Fig. 5*B*). Therefore, it was concluded that the second proline-rich motif of RICH-1 mediates the interaction with CIP4.

In Vitro RhoGAP Activity of RICH-1 and RICH-2—To examine the ability of RICH-1 and RICH-2 to stimulate GTP hydrolysis, GST fusion proteins of RICH-1 (amino acid residues 221–489) and RICH-2 (amino acid residues 217–469) were incubated with Rac1, Cdc42, or RhoA preloaded with [γ-^{32}P]GTP, and the GTP that remained bound to the GTPases was measured. The RhoGAP domains of RICH-1 and RICH-2 stimulated GTP hydrolysis of both Rac1 and Cdc42, but not of RhoA, which was refractory to the activities of the RhoGAPs. In contrast, p50^{RhoGAP} was effective against all three GTPases. RICH-2 stimulated GTP hydrolysis of Rac1 and Cdc42 as efficiently as p50^{RhoGAP}, and it appeared to be a more effective GAP than RICH-1 (Fig. 6). The reason for this difference is not clear; it could reflect differences in either the catalytic activity of the proteins or the stability of the GST fusion proteins. To exclude the possibility that RICH-1 RhoGAP domain could catalyze nucleotide exchange of Rac1 and Cdc42, the Rho GTPases were preloaded with [8-^{3}H]GTP, and the GTP that remained bound was measured. No effect on the nucleotide exchange activity could be detected (data not shown).

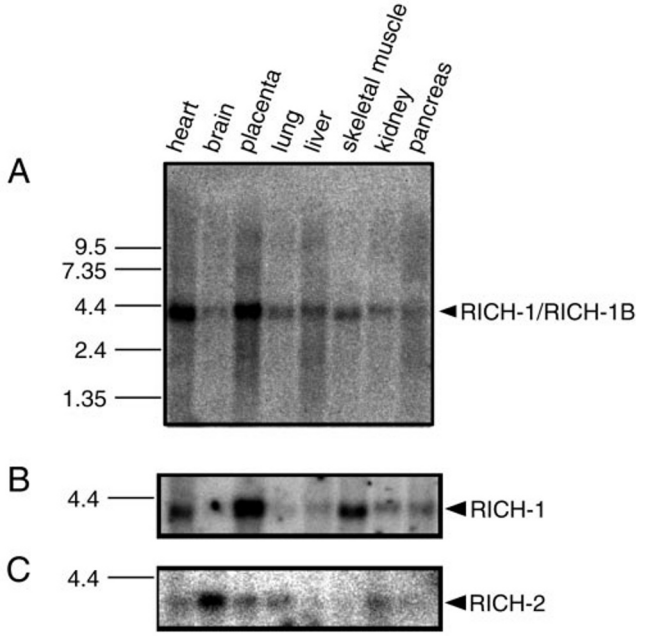

FIG. 2. **Northern blot analysis of mRNA from human tissues as indicated.** *A,* tissue distribution of RICH-1/RICH-1B. *B,* distribution of RICH-1 alone. *C,* distribution of RICH-2 (KIAA0672).

Effect on GTP Loading of Cdc42 and Rac1 by RICH-1—The ability of the RICH-1 RhoGAP domain to regulate the GTP-loaded state of Cdc42 and Rac1 *in vivo* was tested. PAE/PDGFRβ cells were transiently transfected with plasmids encoding either myc epitope-tagged Cdc42 or Rac1 in combination with either plasmids encoding myc epitope-tagged RICH-1 RhoGAP domain or a catalytically inactive R288A mutant RhoGAP domain. GTP-loaded Cdc42 or Rac1 was then collected from lysed cells by GST-WASP-CRIB or GST-PAK1-CRIB, respectively. The simultaneous expression of RICH-1 RhoGAP domain clearly reduced the amount of GTP-Cdc42, whereas the R288A mutant RhoGAP domain had no influence on the GTP loaded status of Cdc42 (Fig. 7*A*). A similar effect was seen for GTP-Rac1, and also in this case, the R288A mutant RhoGAP domain had no effect on GTP-bound Rac1 (Fig. 7*B*). It should be noted that simultaneous expression of the RICH-1 RhoGAP domain and Rac1 resulted in detection of decreased Rac1 expression in the cell lysates. However, under these conditions, no Rac1-GTP could be detected in the GST-PAK1B-CRIB precipitates even after prolonged exposure. The collective data from these experiments and the observations presented in Figs. 6 and 8 suggest that the RICH-1 RhoGAP domain is functional to promote GTP hydrolysis on Cdc42 and Rac1 under *in vivo* conditions.

In Vivo RhoGAP Activity of RICH-1—The ability of the RICH-1 RhoGAP domain to negatively regulate Rac1- and Cdc42-dependent actin rearrangement was tested by transiently transfecting plasmids encoding full-length RICH-1 or the RhoGAP domain into PAE/PDGFRβ cells or Swiss 3T3 fibroblasts. The PAE/PDGFRβ cells were serum-starved for 12 h and then stimulated with 100 ng/ml PDGF-BB for 10 min. PDGF-BB has been shown to have a complex effect on the organization of the actin cytoskeleton. PDGF-BB treatment

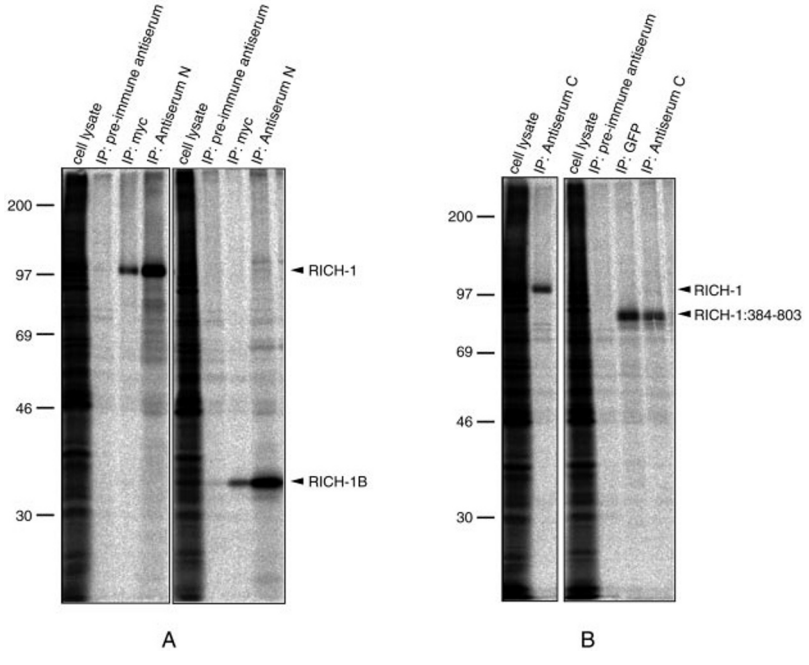

FIG. 3. **Analysis of anti-RICH antiserum.** *A,* myc-tagged RICH-1 or myc-tagged RICH-1B from transiently transfected ^{35}S-labeled Cos-1 cells was immunoprecipitated with either rabbit polyclonal antiserum N or mouse monoclonal anti-myc. *B,* myc-tagged RICH-1 or EGFP-RICH-1:384–803 from transiently transfected ^{35}S-labeled Cos-1 cells was immunoprecipitated with rabbit polyclonal antiserum C or a rabbit polyclonal green fluorescent protein antibody. Antiserum N and antiserum C were rabbit polyclonal antisera raised against an N-terminal peptide and a C-terminal peptide of RICH-1, respectively, as described under "Experimental Procedures."

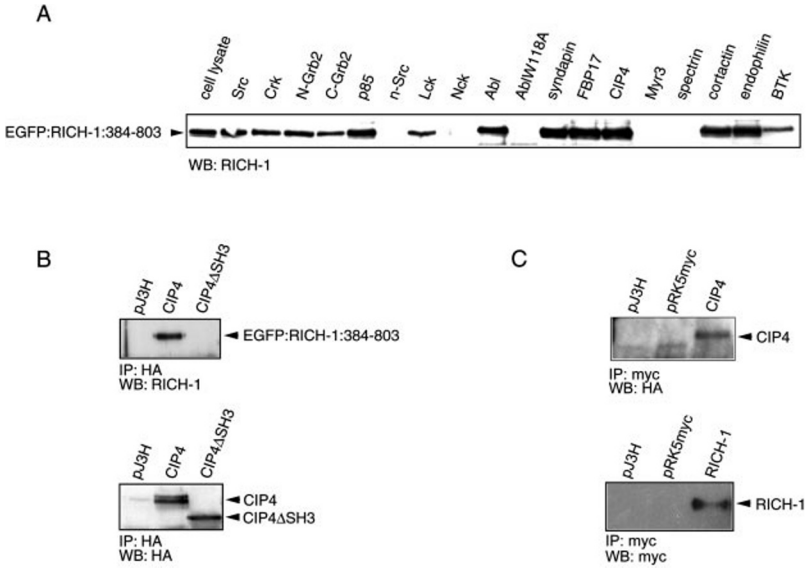

FIG. 4. **Interaction between RICH-1 and SH3 domains.** *A,* interaction of EGFP-tagged RICH-1:384–803 from transiently transfected Cos-1 cells with GST fusion proteins of SH3 domains from Src, Crk, N-Grb2, C-Grb2, p85, n-Src, Lck, Nck, Abl, AblW118A (a mutant unable to bind proline-rich sequences), syndapin, formin-binding protein 17, CIP4, Myr3, spectrin, cortactin, endophilin, and BTK (Bruton's tyrosine kinase). *B,* co-immunoprecipitation of HA-tagged CIP4 or CIP4 lacking the SH3 domain (CIP4ΔSH3) in the pJ3H vector and EGFP:RICH-1:384–803 from transiently transfected Cos-1 cells. EGFP: RICH-1:384–803 was detected by Western blotting using antiserum C, whereas CIP4 and CIP4ΔSH3 were detected by HA antibody. *pJ3H* denotes cells that were transfected with empty vector. *C,* co-immunoprecipitation of HA-tagged CIP4 and myc-tagged RICH-1 in the pRK5myc plasmid. Presence of HA-CIP4 in myc-RICH-1 immunoprecipitate was detected by Western blotting employing a HA-specific antibody. myc-RICH-1 was detected employing a myc-specific antibody; *pJ3H* and *pRK5myc* denote cells transfected with empty vectors.

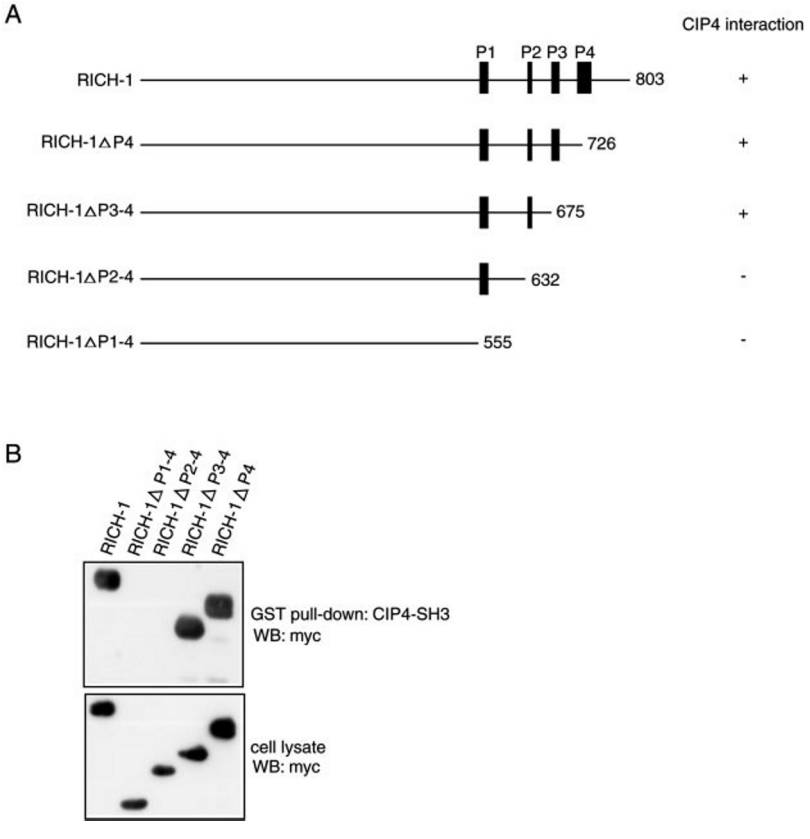

FIG. 5. **Interaction between RICH-1 poly-proline deletion mutants and CIP4.** GST-CIP4-SH3 domain pull-down of myc-RICH-1, myc-RICH-1ΔP4 (residues 1–726), myc-RICH-1ΔP3–4 (residues 1–675), myc-RICH-1ΔP2–4 (residues 1–632), or myc-RICH-1ΔP1–4 (residues 1–555) from transiently transfected Cos-1 cells. Presence of myc-tagged RICH-1 mutants in GST-CIP4-SH3 domain precipitates was detected by Western blotting employing a myc-specific antibody.

results in loss of stress fibers and the formation of lamellipodia (38). These effects are dependent on the activities of both Cdc42 and Rac1 (3, 4). The cells expressing full-length RICH-1 (Fig. 8*A*) or the RhoGAP domain (Fig. 8*B*) were unable to form lamellipodia, in contrast to the surrounding nontransfected cells, which displayed lamellipodia. This suggested that RICH-1 inactivated the endogenous Cdc42 and Rac1 in these cells. This notion was further emphasized by counting the cells, which were scored for the appearance of lamellipodia. A total of 31% of the surrounding cells displayed lamellipodia, in contrast to 9% of the GAP domain-expressing cells and 11% of the RICH-1-expressing cells.

To confirm that the effect on lamellipodia formation was not caused by transfection conditions, catalytically inactive R288A

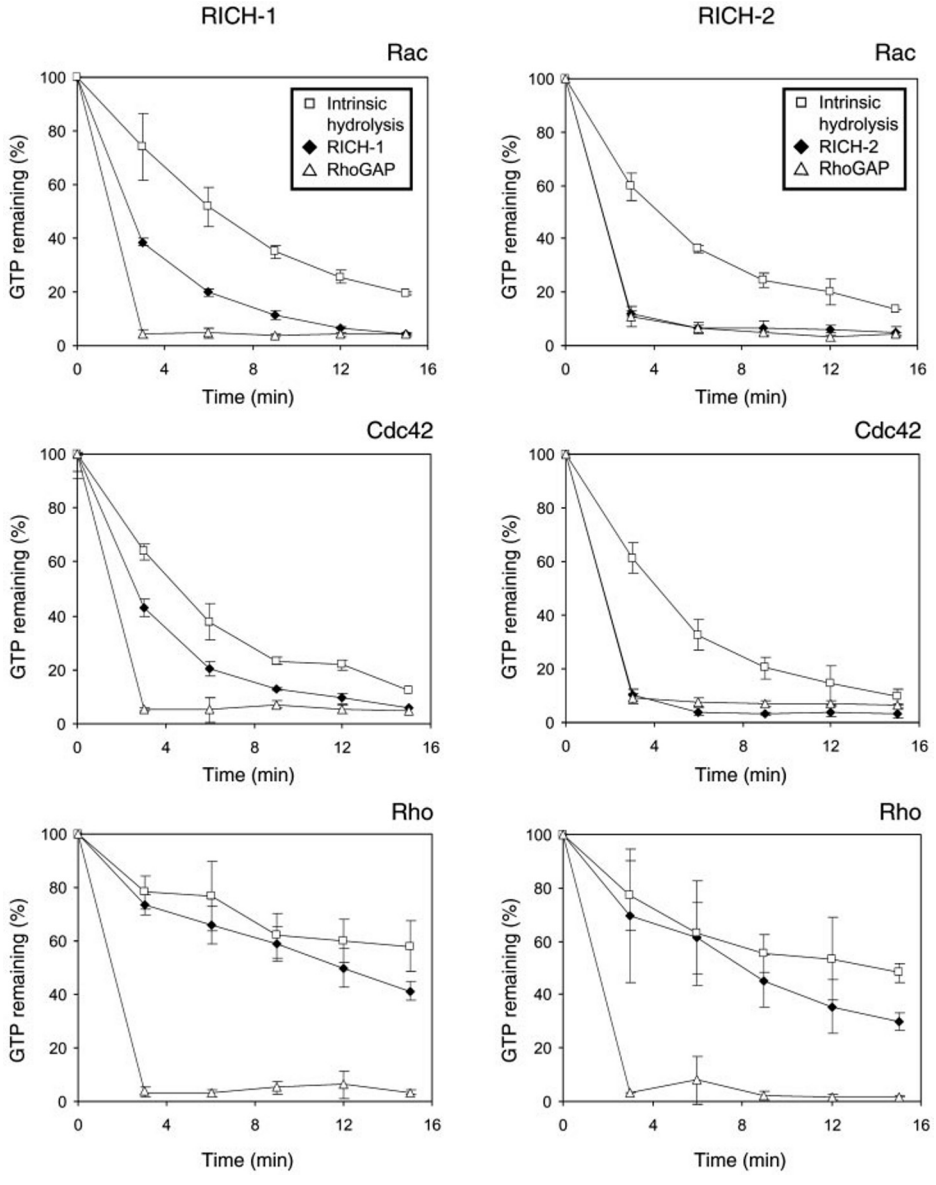

FIG. 6. ***In Vitro* GAP activity.** GTPase activation of Cdc42, Rac1, and RhoA stimulated by the RhoGAP domains of RICH-1, RICH-2, and $p50^{RhoGAP}$, and the intrinsic GTPase activity of the GTPases. A value of 100% corresponds to the initial input of ^{32}P. Each measurement represents the means of three readings.

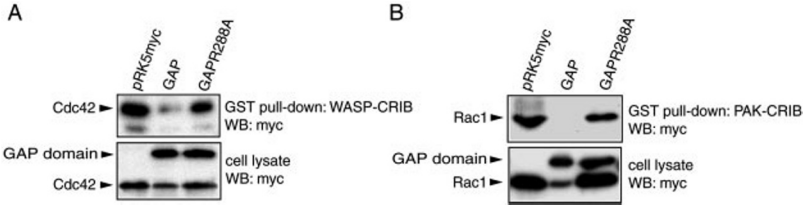

FIG. 7. **Determination of GTP loading of Cdc42 and Rac1.** The amount of active, GTP-loaded Cdc42 and Rac1 was determined by GST pull-down assays employing GST-WASP-CRIB or GST-PAK-CRIB to precipitate GTP-loaded Cdc42 and Rac1 from PAE/PDGFRβ cells transiently transfected with myc-tagged Cdc42 or Rac1 together with either the myc-tagged RICH-1 RhoGAP domain or the GAP-deficient R288A mutant RICH-1 RhoGAP domain. myc-Cdc42 and myc-Rac1 were detected by Western blotting with a myc-specific antibody. The experiment was repeated three times with similar results.

mutant RICH-1 and RICH-1 RhoGAP domain were expressed in PAE/PDGFRβ cells. As expected, expression of these mutant proteins could not abolish lamellipodia formation (Fig. 8, *C* and *D*). This was emphasized by counting the cells showing lamellipodia. A total of 40% of the cells expressing the R288A mutant RhoGAP domain and 37% of the cells expressing full-length RICH-1R288A had lamellipodia. Neither the RhoGAP domain of RICH-1 nor the full-length RICH-1 had any effect on stress fiber formation triggered by the addition of 5% serum to starved Swiss 3T3 cells, which is a response that requires the activity of Rho (Fig. 8, *E* and *F*). This finding further emphasizes the specificity of RICH-1 to function as a GAP for Cdc42 and Rac1, but not for RhoA, under physiological conditions.

Subcellular Localization of RICH-1 and RICH-1B—None of the antisera raised against RICH-1 were particularly useful for immunostaining of endogenous proteins. For this reason, Swiss 3T3 fibroblasts and PAE/PDGFRβ cells were transiently transfected with expression plasmids encoding myc-tagged RICH-1, RICH1-B, or the RhoGAP domain of RICH-1. The subcellular localization of the proteins in transfected cells was visualized by an antibody against the myc epitope. RICH-1 displayed a uniform cytoplasmic distribution (Fig. 9*A*). No obvious effect on

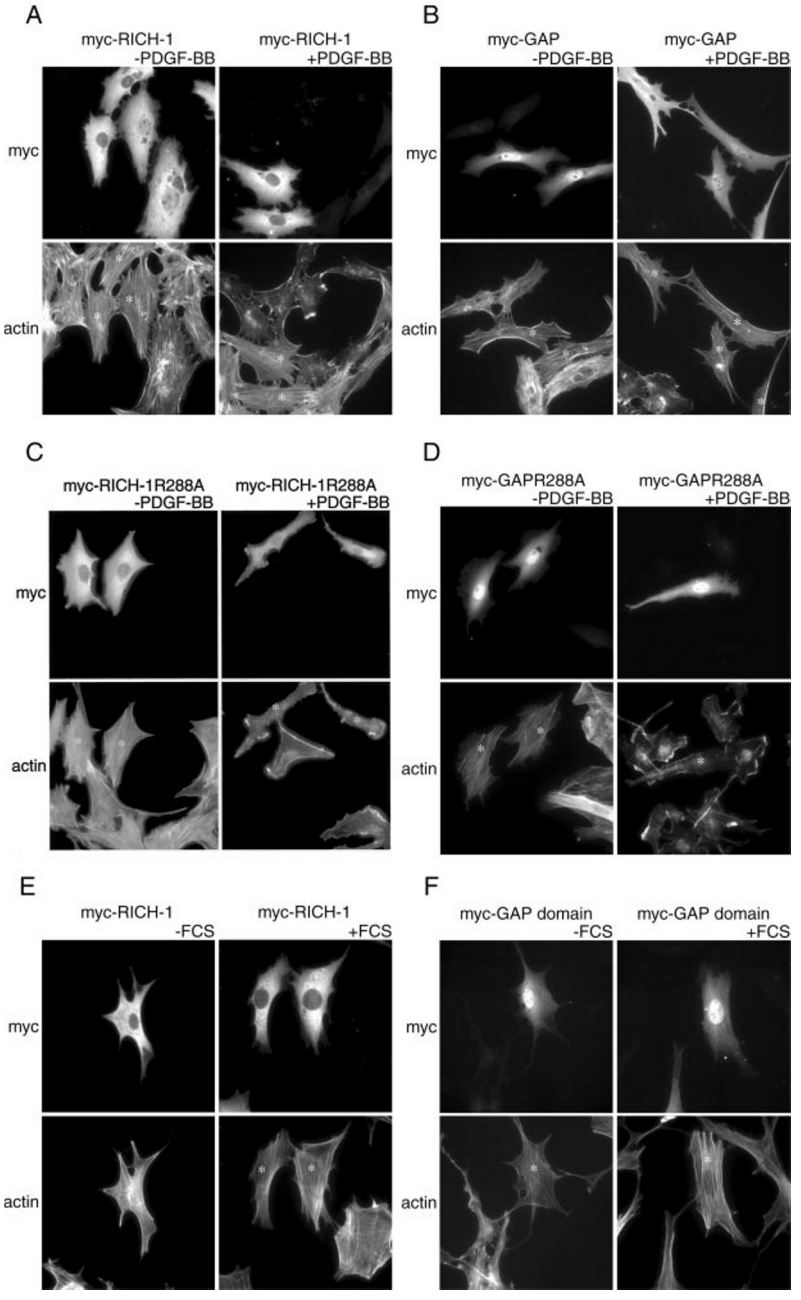

FIG. 8. ***In Vivo* GAP activity of RICH-1.** PAE/PDGFRβ cells transiently transfected with myc-RICH-1 (*A*), myc-RhoGAP domain (*B*), myc-RICH-1R288A (*C*), or myc-GAPR288A (*D*) were serum-starved and remained unstimulated or were stimulated with 100 ng/ml PDGF-BB for 10 min. myc-RICH-1-expressing cells are marked with an *asterisk*. Swiss 3T3 cells transiently transfected with myc-RICH-1 (*E*) or myc-RhoGAP domain (*F*) were serum-starved and remained unstimulated or were stimulated with 5% fetal calf serum for 30 min.

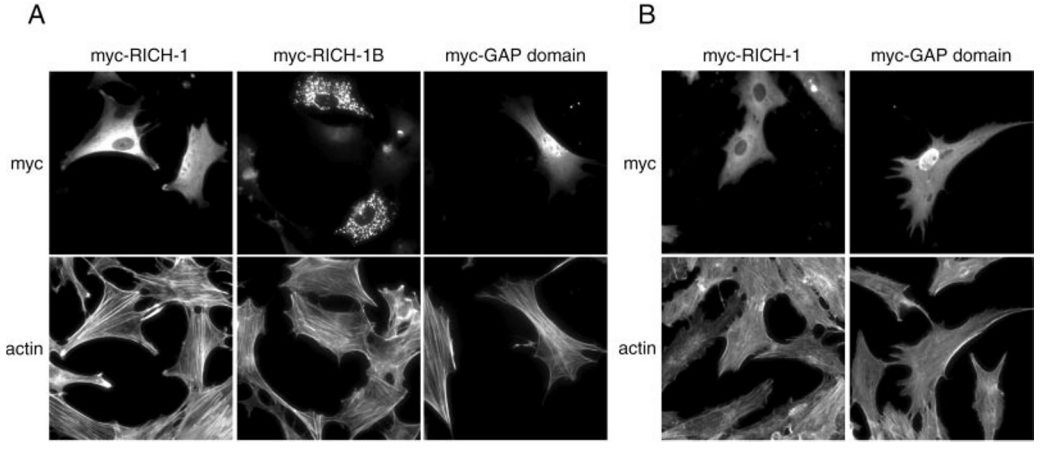

FIG. 9. **Subcellular localization of RICH-1.** *A,* subcellular localization of myc-epitope-tagged RICH-1, RICH-1B, and RICH-1 RhoGAP domain in transiently transfected Swiss 3T3 fibroblasts. *B,* subcellular localization of myc-epitope tagged RICH-1 and RICH-1 RhoGAP domain in transiently transfected PAE/PDGFRβ cells. Subcellular localization of the proteins was detected by myc-specific antibody followed by TRITC-conjugated anti-mouse antibody. Filamentous actin was visualized by using FITC-conjugated phalloidin.

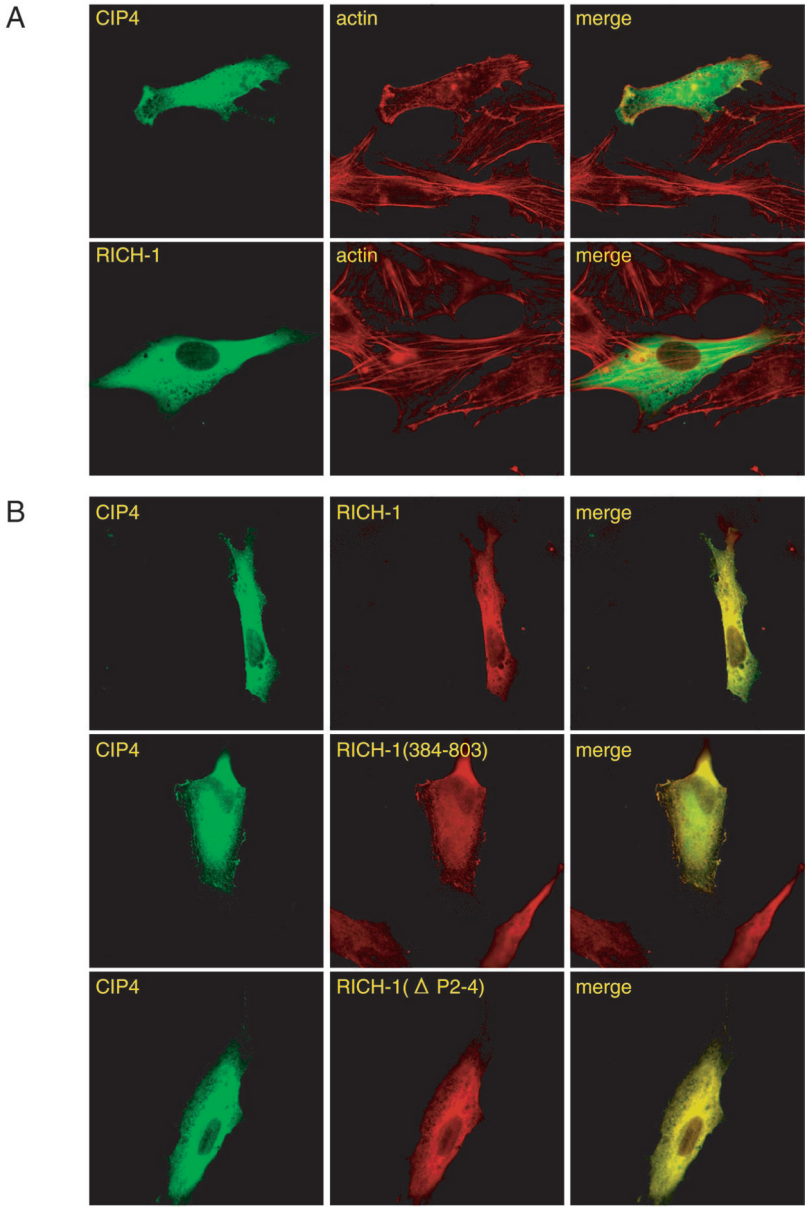

FIG. 10. **Co-localization of RICH-1 and CIP4.** *A,* NIH 3T3 cells were transfected with HA-CIP4 or myc-RICH-1. CIP4 was detected by mouse anti-HA followed by FITC-conjugated anti-mouse antibody. myc-RICH-1 was detected by antiserum N followed by FITC-conjugated anti-rabbit antibody. Filamentous actin was detected by TRITC-conjugated phalloidin. *B,* NIH 3T3 cells were transfected with HA-CIP4 and either myc-RICH-1, EGFP-RICH-1:384–803, or myc-RICH-1ΔP2–4. HA-CIP4 was detected by mouse anti-HA followed by FITC-conjugated anti-mouse antibody. myc-RICH-1 and myc-RICH-1ΔP2–4 were detected by antiserum N followed by TRITC-conjugated anti-rabbit antibody. RICH-1:384–803 was detected by antiserum C followed by TRITC-conjugated anti-rabbit antibody. *C,* NIH 3T3 cells were transfected with myc-L61Cdc42 and HA-CIP4 and either myc-RICH-1, EGFP-RICH-1:384–803, or myc-RICH-1ΔP2–4. HA-CIP4 and the RICH-1 variants were detected as described in *B*.

the organization of the actin filaments could be noticed. The RhoGAP domain was distributed evenly in the cells, including the nucleus. The nuclear localization could be the result of a lack of domain structures that could assist in retaining the protein in the cytoplasm. A similar distribution of myc-RICH-1 and myc-RhoGAP domain was noticed in PAE/PDGFRβ cells (Fig. 9*B*). In contrast to myc-RICH-1, myc-RICH-1B transfected in Swiss 3T3 cells localized to vesicular structures dispersed in the cytoplasm (Fig. 9*A*). This pattern of localization was unique for the RICH-1B splice variant and suggests that the protein has cellular functions distinct from those of RICH-1.

RICH-1 Co-localizes with CIP4 in Vivo—To see whether CIP4 and RICH-1 could localize to the same cellular compartments, HA-CIP4 was expressed alone or together with either myc-RICH-1, EGFP-RICH-1:384–803, or the CIP4 binding-defective myc-RICH-1ΔP2–4 mutant in NIH 3T3 cells. Ectopically expressed HA-CIP4 accumulated in the cell edges, whereas RICH-1 showed a rather uniform cytoplasmic localization (Fig. 10*A*). Simultaneously expressed HA-CIP4 and myc-RICH-1 exhibited a uniform cytoplasmic localization, which made it difficult to visualize a co-localization; however, CIP4 and RICH-1 were frequently seen together in peripheral structures (Fig. 10*B*). Analysis of cells expressing HA-CIP4 and myc-RICH-1:384–803 showed that the proteins co-localized at the cell edges in contrast to HA-CIP4 and myc-RICH-1ΔP2–4, which did not visibly co-localize (Fig. 10*B*).

To further visualize a RICH-1 and CIP4 co-localization, we took advantage of the observation that simultaneous expression of Cdc42 and CIP4 was shown to relocate CIP4 from uniform cytoplasmic distribution into peripheral and dorsal clusters on fibroblasts (25). This prompted us to analyze the ability of RICH-1 to participate in the Cdc42-induced CIP4 relocalization. NIH 3T3 fibroblasts were transfected with plasmids encoding combinations of constitutively active Cdc42, CIP4, and either full-length RICH-1 or the C-terminal portion of RICH-1 or RICH-1ΔP2–4 and then examined for co-localization of CIP4 and the RICH-1 variants. HA-CIP4 was detected by an antibody against the HA tag, whereas RICH-1 or RICH-1ΔP2–4 and RICH-1:384–803 were detected by antiserum N and antiserum C, respectively. As expected, constitutively active Cdc42 induced a relocalization of CIP4, and these clusters also contained RICH-1 (Fig. 10*C*). In NIH 3T3 cells expressing constitutively active Cdc42, CIP4, and the C-terminal portion of RICH-1, CIP4 and RICH-1 colocalized to a larger extent than

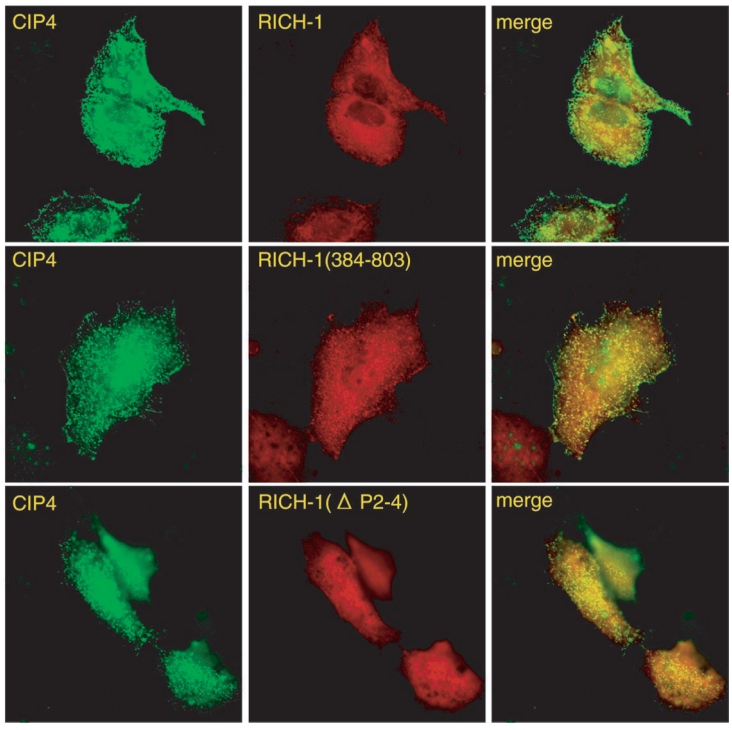

FIG. 10—*continued*

CIP4 and full-length RICH-1 (Fig. 10*C*). This difference might be caused by the absence of endophilin-like and RhoGAP domains in this deletion mutant, which could be postulated to be important for the localization of RICH-1 to specific cellular compartments. As expected, CIP4 defective binding mutant RICH-1ΔP2–4 did not co-localize visibly with CIP4 under these conditions (Fig. 10*C*). These data indicate that CIP4 and RICH-1 can interact inside cells and that the proteins affect the subcellular localization of each other.

DISCUSSION

RICH-1 is a ubiquitously expressed protein and exists in at least two different splice variants, RICH-1 and RICH-1B. The shorter splice variant seems to be the predominant splice variant in neuronal tissue, whereas both RICH-1 and RICH-1B seem to be expressed in B cells and HeLa cells. The intriguing findings that RICH-1 contained a domain with homology to endophilins (35) and that this domain is the only constituent in RICH-1B suggested that this domain has a cellular function. The corresponding domain in members of the endophilin family of proteins has been implicated to function as a lysophosphatidic acid acyl transferase, catalyzing the conversion of lysophosphatidic acid to phosphatidic acid (39). This is thought to alter the three-dimensional structure of the membrane lipids. According to the proposed scenario, this local shape change of the lipids will cause invaginations of the plasma membrane, a process that occurs during clathrin-mediated endocytosis of synaptic vesicles. Interestingly, when ectopically expressed in fibroblasts, RICH-1B was present exclusively in vesicular structures, as opposed to RICH-1, which displayed a more uniform cytoplasmic localization. This might suggest that RICH-1B can have a role in either vesicle formation or membrane trafficking. It remains to be seen whether RICH-1B can display an enzymatic activity similar to that of endophilins and participate in endocytosis or exocytosis.

The RhoGAP domains of RICH-1 and RICH-2 were able to catalyze GTP hydrolysis on Rac1 and Cdc42, but not on RhoA. RICH-1 was furthermore shown to function as a Cdc42- and Rac-specific GAP *in vivo* because cells expressing either full-length RICH-1 or the RhoGAP domain were unable to form membrane ruffles, a phenomenon that requires the activities of Cdc42 and Rac1. Conversely, the Rho-dependent serum-induced stress fibers remained unaffected. These observations are consistent with previous reports on the related RhoGAP 3BP-1, which was shown to be a GAP for Rac1, Rac2, RhoG, and Cdc42Hs but not for TC10, RhoA, RhoB, or RhoC *in vitro* (36). Microinjection of 3BP-1 in fibroblasts interfered with the PDGF-induced membrane ruffles.

Overexpression, either by means of ectopic expression or microinjection of RhoGAP proteins, has been a general and successful method to evaluate RhoGAP activities under physiological conditions. In this way, $p190^{RhoGAP}$, p122, and GRAF (GTPase regulated associated with focal adhesion kinase) were shown to be specific for Rho because they were able to abrogate serum- or sphingosine-1-phosphate-induced formation of stress fibers (40–42). Furthermore, microinjection of CdGAP inhibited the formation of bradykinin-induced filopodia, a response that requires the activity of Cdc42 (43). The importance of this kind of analysis for the establishment of *in vivo* function can be further exemplified by $p50^{RhoGAP}$. This protein is a RhoGAP primarily for Cdc42 and, to a lesser extent, for Rac and Rho *in vitro*. However, when microinjected in fibroblasts, it inhibited the serum-induced formation of stress fibers but had no effect on PDGF-induced membrane ruffling (44). This demonstrates that the *in vitro* specificity does not necessarily overlap with the specificity *in vivo*. RhoGAP domain-containing proteins can furthermore function as effectors, transducing additional signals downstream of Rho GTPases. Work on the Rac GAP n-Chimaerin showed that microinjection of the protein in fibroblasts and neuroblastoma cells induced a membrane ruffling activity (44). This effect was dependent on the ability of n-Chimaerin to bind to Rho GTPases, but not on the GAP activity of the protein (45). To date, more than 20 distinct RhoGAP domain-containing proteins have been identified compared with only 4 potential RasGAPs (6, 7); moreover, sequence information from the Human Genome Project indicates the presence of several as yet uncharacterized RhoGAPs.[3] The

[3] N. Richnau and P. Aspenström, unpublished observation.

reason for this richness of RhoGAPs is not clear, but it might be partially explained by the abundance of Rho GTPases as compared with Ras GTPases. Another explanation might reside in the fact that RhoGAP proteins are multivalent signaling modules that, in addition to their GAP domains, contain pleckstrin homology domains, proline-rich domains, Dbl homology domains, Src homology 2 domains, SH3 domains, myosin-like domains, serine/threonine kinase domains, and so forth (6, 7). This demonstrates that members of this large family of proteins participate in a multitude of signaling pathways.

RICH-1 was found to interact specifically with the SH3 domain of CIP4. CIP4 was originally found in a yeast two-hybrid system screen for Cdc42-interacting proteins (25). In this report, it was noticed that overexpression of CIP4 in Swiss 3T3 fibroblasts caused a loss of actin filament bundles. Moreover, the concomitant expression of CIP4 and activated mutants of Cdc42 resulted in a relocalization of CIP4 into clusters at the cell periphery and the dorsal side of the cells. Ectopically expressed RICH-1 was also found to localize to the CIP4-containing clusters; however, the function of RICH-1 in these structures is currently unknown. In addition to binding to RICH-1, the SH3 domain of CIP4 has been shown to bind to WASP, and this interaction has been proposed to be important for a CIP4-induced relocalization of WASP to the microtubule system (46).

Several CIP4-related proteins have been identified, including formin-binding protein 17 (47) and Cdc15. The latter protein is the prototype of a family of CIP4 relatives that involve a number of homologous mammalian proteins (48). Cdc15 was originally found in *Schizosaccharomyces pombe*, where *cdc15* mutant cells are defective in cytokinesis; more specifically, they are defective in forming the cleavage furrow necessary for the partitioning of the dividing cells (49). The mammalian Cdc15 includes the PEST phosphatase-binding protein PSTPIP (50) and the FAP52/syndapin proteins (51, 52). In conformity with CIP4, PSTPIP and syndapin have also been found to bind members of the WASP family of proteins (52–54). However, the role of these interactions in the function of WASP is currently unclear. In summary, CIP4 and CIP4-related proteins participate in signaling pathways that regulate cytoskeletal reorganizations and intracellular transport, and it is likely that RICH-1 and RICH-2 participate in these signaling pathways.

Acknowledgments—GST fusion constructs of SH3 domains were generous gifts from M. Bähler (Myr3), J. T. Parsons (cortactin), L. Brodin (endophilin), A.-M. Pendergast (Abl), L. Backman (spectrin), P. Chavrier (Btk), and I. Dikic (Src, Crk, Grb2, p85, n-Src, Lck, and Nck). We thank Carl-Henrik Heldin for critical reading of the manuscript.

REFERENCES

1. Mitchison, T. J., and Cramer, L. P. (1996) *Cell* **84,** 371–379
2. Schmidt, A., and Hall, M. N. (1998) *Annu. Rev. Cell Dev. Biol.* **14,** 305–338
3. Hall, A. (1998) *Science* **279,** 509–514
4. Van Aelst, L., and D'Souza-Schorey, C. (1997) *Genes Dev.* **11,** 2295–2322
5. Whitehead, I. P., Campbell, S., Rossman, K. L., and Der, C. J. (1997) *Biochim. Biophys. Acta* **1332,** F1–F23
6. Lamarche, N., and Hall, A. (1994) *Trends Genet.* **10,** 436–440
7. Zalcman, G., Dorseuil, O., Garcia-Ranea, J. A., Gacon, G., and Camonis, J. (1999) *Prog. Mol. Subcell. Biol.* **22,** 85–113
8. Sasaki, T., and Takai, Y. (1998) *Biochem. Biophys. Res. Commun.* **245,** 641–645
9. Aspenström, P. (1999) *Exp. Cell Res.* **246,** 20–25
10. Vignal, E., De Toledo, M., Comunale, F., Ladopoulou, A., Gauthier-Rouvière, C., Blangy, A., and Fort, P. (2000) *J. Biol. Chem.* **275,** 36457–36464
11. Kjøller, L., and Hall, A. (1999) *Exp. Cell Res.* **253,** 166–179
12. Mackay, D. J. G., and Hall, A. (1998) *J. Biol. Chem.* **273,** 20685–20688
13. Gómez, J., Martínez-A, C., González, A., and Rebollo, A. (1998) *Immunol. Cell Biol.* **76,** 125–134
14. Aspenström, P. (1999) *Curr. Opin. Cell Biol.* **11,** 95–102
15. Bishop, A. L., and Hall, A. (2000) *Biochem. J.* **348,** 241–255
16. Pollard, T. D., Blanchoin, L., and Mullins, R. D. (2000) *Annu. Rev. Biophys. Biomol. Struct.* **29,** 545–576
17. Zigmond, S. H. (2000) *J. Cell Biol.* **150,** 117–120
18. Snapper, S. B., and Rosen, F. S. (1999) *Annu. Rev. Immunol.* **17,** 905–929
19. Derry, J. M., Ochs, H. D., and Francke, U. (1994) *Cell* **78,** 635–644
20. Ochs, H. D. (1998) *Springer Semin. Immunopathol.* **19,** 435–458
21. Burbelo, P. D., Drechsel, D., and Hall, A. (1995) *J. Biol. Chem.* **270,** 29071–29074
22. Burbelo, P. D., Snow, D. M., Bahou, W., and Spiegel, S. (1999) *Proc. Natl. Acad. Sci. U. S. A.* **96,** 9083–9088
23. Joberty, G., Perlungher, R. R., and Macara, I. G. (1999) *Mol. Cell. Biol.* **19,** 6585–6597
24. Pirone, D. M., Fukuhara, S., Gutkind, J. S., and Burbelo, P. D. (2000) *J. Biol. Chem.* **275,** 22650–22656
25. Aspenström, P. (1997) *Curr. Biol.* **7,** 479–487
26. Cicchetti, P., Mayer, B. J., Thiel, G., and Baltimore, D. (1992) *Science* **257,** 803–806
27. Aspenström, P., and Olson, M. F. (1995) *Methods Enzymol.* **256,** 228–241
28. Sambrook, J., Fritsch, E. F., and Maniatis, T. (1989) *Molecular Cloning: A Laboratory Manual* 2nd Ed., Cold Spring Harbor Laboratory, Cold Spring Harbor, NY
29. Short, J. M., Fernandez, J. M., Sorge, J. A., and Huse, W. D. (1988) *Nucleic Acids Res.* **16,** 7583–7600
30. Self, A. J., and Hall, A. (1995) *Methods Enzymol.* **256,** 3–10
31. Self, A. J., and Hall, A. (1995) *Methods Enzymol.* **256,** 67–76
32. Kriegler, M. (1990) *Gene Transfer and Expression: A Laboratory Manual*, W. H. Freeman and Company, NY
33. Ren, X.-D., and Schwartz, M. A. (2000) *Methods Enzymol.* **325,** 264–272
34. Kozak, M. (1991) *J. Biol. Chem.* **266,** 19867–19870
35. Ringstad, N., Nemoto, Y., and De Camilli, P. (1997) *Proc. Natl. Acad. Sci. U. S. A.* **94,** 8569–8574
36. Cicchetti, P., Ridley, A. J., Zheng, Y., Cerione, R. A., and Baltimore, D. (1995) *EMBO J.* **14,** 3127–3135
37. Yu, H., Chen, J. K., Feng, S., Dalgarno, D. C., Brauer, A. W., and Schreiber, S. L. (1994) *Cell* **76,** 933–945
38. Eriksson, A., Siegbahn, A., Westermark, B., Heldin, C.-H., and Claesson-Welsh, L. (1992) *EMBO J.* **11,** 543–550
39. Schmidt, A., Wolde, M., Thiele, C., Fest, W., Kratzin, H., Podtelejnikov, A. V., Witke, W., Huttner, W. B., and Söling, H.-D. (1999) *Nature* **401,** 133–141
40. Chang, J.-H., Gill, S., Settleman, J., and Parsons, S. J. (1995) *J. Cell Biol.* **130,** 355–368
41. Sekimata, M., Kabuyama, Y., Emori, Y., and Homma, Y. (1999) *J. Biol. Chem.* **274,** 17757–17762
42. Taylor, J. M., Macklem, M. M., and Parsons, J. T. (1999) *J. Cell Sci.* **112,** 231–242
43. Lamarche-Vane, N., and Hall, A. (1998) *J. Biol. Chem.* **273,** 29172–29177
44. Ridley, A. J., Self, A. J., Kasmi, F., Paterson, H. F., Hall, A., Marshall, C. J., and Ellis, C. (1993) *EMBO J.* **12,** 5151–5160
45. Kozma, R., Ahmed, S., Best, A., and Lim, L. (1996) *Mol. Cell. Biol.* **16,** 5069–5080
46. Tian, L., Nelson, D. L., and Stewart, D. M. (2000) *J. Biol. Chem.* **275,** 7854–7861
47. Chan, D. C., Bedford, M. T., and Leder, P. (1996) *EMBO J.* **15,** 1045–1054
48. Lippincott, J., and Li, R. (2000) *Microsc. Res. Tech.* **49,** 168–172
49. Fankhauser, C., Reymond, A., Cerutti, L., Utzig, S., Hofmann, K., and Simanis, V. (1995) *Cell* **82,** 435–444
50. Spencer, S., Dowbenko, D., Cheng, J., Li, W., Brush, J., Utzig, S., Simanis, V., and Lasky, L. A. (1997) *J. Cell Biol.* **138,** 845–860
51. Meriläinen, J., Lehto, V.-P., and Wasenius, V.-M. (1997) *J. Biol. Chem.* **272,** 23278–23284
52. Qualmann, B., Roos, J., DiGregorio, P. J., and Kelly, R. B. (1999) *Mol. Biol. Cell* **10,** 501–513
53. Wu, Y., Spencer, S. D., and Lasky, L. A. (1998) *J. Biol. Chem.* **273,** 5765–5770
54. Qualmann, B., and Kelly, R. B. (2000) *J. Cell Biol.* **148,** 1047–1062